

Experimental Analysis of Autogenous Healing in Early Stage of Concrete

Chandra Shekher Giri* and Pankaj Kumar Singh**

ABSTRACT

Autogenous healing is mostly produced by continuous hydration or carbonation. In this investigation, the autogenous healing-induced fracture closure for young concrete will be quantified. Three different healing scenarios—water immersion, a humidity chamber, and wet/dry cycles—as well as two crack sizes—0.1 mm and 0.4 mm—were employed to measure the healing. The fracture closure was evaluated after 7, 14, 28, and 42 days of recovery. The internal state of the cracks was verified using phenolphthalein and visual inspection. The results show that whereas specimens housed in a humidity room did not show healing, specimens exposed to wet/dry cycles and water immersion completely sealed tiny fissures (under 0.15 mm). Although autogenous healing performed more quickly during wet/dry cycles, submersion had a bigger overall impact. But when the specimens' interiors were examined, it became clear that the majority of the self-closing occurred on the surface and that carbonation in the crack faces was really only perceptible very close to the specimen's surface. Additionally, a preliminary strategy to forecast fracture closure during autogenous healing in concrete is suggested by this work.

Keywords: *Cement Concrete; Autogenous Healing; Compressive Strength.*

1.0 Introduction

Self-healing concrete is an unique type of concrete that can repair itself on its own, typically by filling in cracks [1]. The self-healing phenomenon known as autogenous healing can occur naturally even in concrete, which was not designed with self-healing in mind, according to reports in the literature [1-3]. Recently, specific products and technologies have been developed to promote or improve this trait (autonomous healing) [1-3]. The carbonation of calcium hydroxide or the continuing hydration of unhydrated cement particles are the main mechanisms that cause autogenous healing [3]. The latter is often regarded as the phase that has the most impact on autogenous healing [4]. Calcium carbonate, $\text{Ca}(\text{CO}_3)$, is produced when carbon dioxide from water and calcium ions from portlandite, $\text{Ca}(\text{OH})_2$, interact.

In order to analyse concrete autogenous healing, one of the early studies in this field to be published [4] looked at the water permeability of cracked concrete in the presence of water. It was shown that calcium carbonate precipitation from crack filling was the main contributor to the restoration of watertightness (calcite). Although continuing hydration and carbonation can have an effect on the process, the former has a stronger impact on the early stages of self-healing and the latter at later stages [5]. This is true despite the critical function that carbonation plays in producing autogenous repair.

*Corresponding author; M.Tech Research Scholar, Department of Civil Engineering, KNIT Sultanpur, Uttar Pradesh, India (E-mail: giri.ucem@gmail.com)

**M.Tech Research Scholar, Department of Civil Engineering, KNIT Sultanpur, Uttar Pradesh, India (E-mail: pankaj02021992@gmail.com)

Autogenous healing is divided into two phases with separate behaviours, surface-controlled phase and diffusion-controlled phase, according to findings [4]. The first phase is controlled by the reaction between calcium ions at the crack's surface and those in the water inside the fracture, which results in the formation of a layer of calcium carbonate. When the calcium carbonate layer prevents calcium ions from coming into direct contact with water, the process depends on the transport of ions from the concrete to the fracture through that layer. The second phase officially starts at this point. Within the first three to five days of interaction with the water flow, the first phase, which involves crystal growth and crack width reduction, would take place. The same study [4] discovered that water permeability reduced and crystal formation only happened very slowly during the first week of healing. Recent research indicates that autogenous healing under water occurs more quickly during the first month of recovery [6], but stops or considerably slows down after 1-2 [7,8] or after 3-5 [6] months.

A crack's age and the efficiency of autogenous healing have been compared in some studies.

Early-age cracks demonstrated a higher autogenous healing efficiency than older cracks, according to one study [7]. The study measured the size of the fissures at 20, 24, 48, and 72 hours. Another study [9] examined cracks that appeared at ages 3 and 28 days and discovered that smaller cracks healed more rapidly and easily than larger ones. Specifically, early-age cracks under 0.05 mm mended in 12 days, those between 0.1 and 0.2 mm in 29 days, and those between 0.2 and 0.3 mm in 44 days thanks to autogenous repair. Larger fractures, on the other hand, remained open, and 28-day cracks only completely sealed for cracks under 0.05 mm in 12 days. Regarding older cracks, the authors of [6] studied 28-day and 6-month-old cracks. It was shown that although the effectiveness of crack healing reduced with age, the changes were insignificant, probably because the newborns had advanced hydration at one month.

Water must be available in order for autogenous healing to take place, thus ensuring sure it is crucial. Some studies [7,10] or [11] looked at how relative humidity or air-water curing compared, or both (60 percent, 95 percent, and water immersion). They discovered that specimen healing under water immersion had a better reaction when comparing the outcomes of specimen healing in humidity chambers with air curing. Recent studies [12] showed that Engineered Cementitious Composite (ECC) specimens healing in CO₂-rich-water conditions generated the strongest self-healing performance when compared to air, underwater, and CO₂-rich-air healing circumstances. In that case, the creation of calcium carbonate made it possible for cracks with a diameter of 0.458 mm to heal completely within 30 days (CaCO₃). In a different study [13], calcium silicate hydrate and calcium carbonate precipitates were discovered inside the crack, enhancing the efficacy of crack healing. This study looked at the repair of concrete in water containing minute silica particles.

According to several studies [14,15], entire immersion generated better results than alternating wet/dry cycles in terms of recovering water tightness and fracture closing, with wet/dry cycles having a higher dispersion. However, studies have shown that wet/dry cycling settings promote healing more effectively than complete submersion in water [16–18]. Studies [16,17] carried out on ECC specimens showed that regimes with different moisture conditions did not induce significant healing as measured by resonant frequency, but water immersion or combination cycles did. They also claimed that the combined cycles conditions delivered the optimum results.

Many methods for evaluating the self-healing properties of concrete have recently been developed in an effort to standardise them. A public standard, however, has not yet been released. By the type of property being studied—transport properties, mechanical properties, filling of cracks,

etc.—different methodologies have been used to evaluate the improvements brought about by the healing process. Although some studies [9,19,20] have used crack closure as the major indicator of self-healing, the easiest way to assess self-healing is to look at surface cracks. As a result, it has frequently been used as an additional technique to visually confirm the results of other tests.

This study’s objective is to quantify the amount of early-age concrete crack closure brought on by autogenous healing in fractures of two distinct sizes, one centred around 0.1 mm and the other around 0.4 mm. These two crack sizes represent what are typically thought of as being somewhat above and below service conditions, respectively. In this study, crack closure is examined in three distinct healing scenarios: water immersion, wet/dry cycles, and a humidity chamber. When autogenous healing is absent, the latter is employed as a reference scenario. Numerous methods are used to measure autogenous healing, and an early crack closure model is looked into. Since carbonation is usually believed to be the fundamental process that leads to autogenous healing, the inside condition of the fracture is also visually and phenolphthalein-evaluated.

2.0 Experimental Setup

2.1 Materials

In this study, autogenous healing in C30/37 strength concrete is investigated. The cement used was CEM I 42.5 R from Lafarge, which had no mineral additives because their presence could affect the healing processes. Even though huge particles may prevent self-healing, concrete with coarse aggregate was tested to see how it would do in a situation more akin to real projects. The coarse aggregates were crushed calcareous aggregates with diameters (dmin/Dmax) of 7/12 and 4/7 mm. As the fine aggregate, calcareous sand from nature was used. Limestone powder was added to modify the aggregates’ size distribution and create a more continuous particle distribution curve.

To create a mixture with an S3 consistency class, superplastizer Sika ViscoCrete-5980 had to be added. Steel fibres, which had previously been utilised effectively in [15], were added in a quantity of 40 kg/m³ (0.51 percent by volume) in order to manage the crack width during the precracking and healing periods. Bekaert produced Dramix® RC 65/35 BN fibres that were 0.55 mm thick and 35 mm long around the diameter. Table 1 shows the concrete dosage that was used in this study.

Table 1: Concrete Mix Proportions and Characterization Properties

Constituent	Quantity (kg/m ³)
Cement CEM I 42.5 R	275
Water	165
Gravel (4–12 mm)	908
Natural sand	988
Limestone powder	50
Superplasticizer	5
Steel fibers	40
Slump (mm)	145
Avg. Compression strength (MPa)	38.3

Cylindrical specimens with diameters ranging from 150 mm to 300 mm were cast in conformity with UNE-EN 12390-2. The specimens were cast, let to cure in the mould for 24 hours, and then kept in a humidity room at standard conditions (20 °C and >95 percent relative humidity) until it was time for testing. According to EN 12390-3, three cylinders were used to measure the concrete’s compressive strength at 28 days, and an EN 12350-2 slump test was utilised to gauge the

batch's consistency. The slump was 145 mm, the average compression strength was 38.3 MPa, and the consistency class was S3. The results of these characterizations are shown in Table 1.

Circular saws were used to cut concrete sample in half. The last samples gathered for the crack closing evaluation were those with dimensions of 150 mm by 150 mm. The edge sides of each resulting cylinder were polished to eliminate mortar layers on the bottom surface in contact with the moulds and asperities on the top free surface of the specimen as cast. This process allowed us to evaluate whether a fracture hit and fractured an aggregate or if it penetrated cement paste. A smooth surface aids in a better evaluation of crack closing.

The tiny cylindrical concrete examples had already started to break at two days old. Two levels of cracks—0.1 and 0.4 mm—were created for the splitting test. Steel fibres added to the mixture enabled the control and subsequent maintenance of crack width. All specimens were given permission to heal at the age of 3 days across 42 days. The crack widths were measured at 0, 7, 14, 28, and 42 days after healing.

Three environmental exposure parameters were considered in order to establish the effect of water availability on the analysed specimens' capacity for self-healing:

- W/D (wet/dry cycles): immersion in tap water at a temperature of 15 C for 3.5 days and air exposure for an additional 3.5 days (air conditions: relative humidity: >95 percent);
- WI (water immersion): continuous immersion in tap water at a temperature of 15 1 C, only adding water to account for evaporation and to maintain a constant water level.

The fracture was kept in a lateral position on specimens under the three healing conditions to ensure comparability. A total of 18 cylindrical concrete specimens were precracked during the splitting test, resulting in two cracks per specimen. We looked at a total of 36 cracks. Since these specimens were distributed evenly over the three healing exposures, twelve cracks were examined in each healing exposure. Due to the fact that they were taken at 0, 7, 14, 28, and 42 days after the injury, a total of 180 photographs were analysed for this investigation.

2.2 Precracking methodology

At the age of two days, cylindrical specimens were precracked using a splitting test (Figure 1 Left) to achieve two goal values of crack width that were managed using a calibration ruler.

Figure 1: Precracking by Splitting Test (Left) and USB Microscope to Analyze Cracks (Right)



Investigated crack width levels were 0.1 and 0.4 mm. The former was chosen as a value that is permitted in structural codes, even in XS hazardous environments, whilst the later was chosen as a high crack level among those authorised in the regulations.

The use of fibres allowed for a cracking control that was sufficient to discern between the two planned fracture levels with tolerable variability, despite the fact that there is an inherent dispersion when using a reference ruler due to the human component. The average size was 0.10 mm with a standard deviation of 0.04 mm for the group with cracks measuring 0.1 mm and 0.4 mm, and for both groups, the average size was 0.38 mm with a standard deviation of 0.08 mm.

This method offers a crude method of managing the crack width and allows for the cracking of more specimens in an acceptable length of time. It is also reasonably simple.

2.3 Crack width measurement

This study used an optical USB microscope (PCE-MM200) from PCE Instruments, Albacete, Spain, to show cracks on a computer in real time. The microscope uses LEDs as a light source and to provide superb images (Figure 1 Right). Before each set of readings, the measurements were checked for accuracy using a crack width ruler and the PCE-MM 200 programme on the microscope. Each image is 1600 x 1200 pixels in size and has a 96 ppp resolution. Using Adobe Photoshop CS6, the photos were inspected to estimate each fracture’s size (Adobe, San Jose, CA, USA). The crack’s width was measured in the geometric centre of the cylinder’s section.

Photographs were collected before and after each healing interval to evaluate autogenous healing. Before taking pictures, all of the concrete samples were cleaned with compressed air to remove any dust contaminants. The specimens that had been healing throughout the preceding days in water immersion were allowed to dry for two hours in the lab to produce a dry surface. The LEDs would reflect light in the breach if there was no water present.

It was common practise to evaluate self-healing by crack closure using Equation (1):

$$\text{Crack closing rate} = 1 - \omega_t / \omega_0 \quad \dots(1)$$

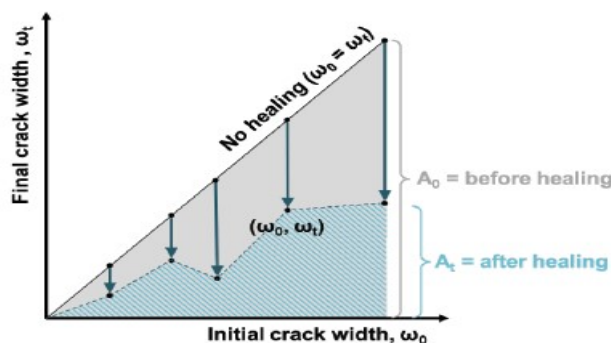
where ω_0 is the initial crack width (mm)—in this study, measured after precracking—and ω_t is the final crack width (mm)—in this study, measured after a healing period of t days ($t = 7, 14, 28$ and 42 days). This equation has been previously used by several authors ([15,21,22], among others).

According to other studies [9,19,23], a self-healing index might be used to assess a global value. Each crack width measurement for a certain type of concrete is considered, along with how that measurement has evolved over time, to construct this index. B is calculated using the formula in Equation (2), and the conceptual picture is displayed in Figure 2:

$$\beta = 1 - A_t / A_0 \quad \dots(2)$$

where A_0 is the area between the bisecting line and the horizontal axis, and A_t is the area between the polyline that unites all the remaining crack width points and the horizontal axis (blue diagonal stripes in Figure 2).

Figure 2: Concept for the Evaluation of a Global Crack Closing, Following the Methods used in [9,19]



The maximum fracture widths taken into account must be as comparable as is practical given that the beginning region before to healing A_i must be comparable in each of the cases being examined. The study's greatest crack widths for the humidity chamber, wet/dry cycles, and submersion in water were 0.48 mm, 0.44 mm, and 0.45 mm, respectively. As a result, the results are regarded as equal.

Three different methods will be used in this study to evaluate the crack closure: (1) direct investigation of the crack width evolution; (2) crack closing rate; and (3) the designated self-healing index.

2.4. Internal crack and carbonation

In many cases, the cracks were completely sealed. Using a concrete circular saw, these restored samples were cut transversally into two halves to examine the internal state of the fissures. Since it is thought that continuing hydration and carbonation are the main causes of the reactions, phenolphthalein was used as an indication to determine whether carbonation happened. After being cut, the samples were allowed to cure for 30 minutes before having phenolphthalein sprayed on their surfaces. Additional samples from earlier trials were examined in order to fully verify this claim; in particular, these were samples that had recovered after being buried in water at 30 °C for six months in order to maximise self-healing [24].

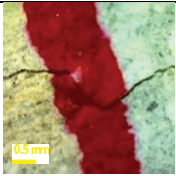
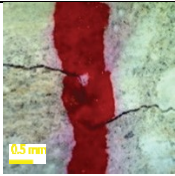
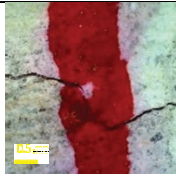
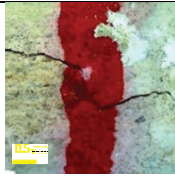
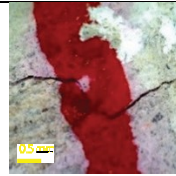
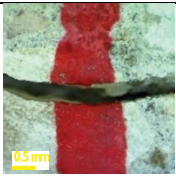


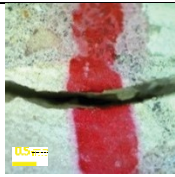
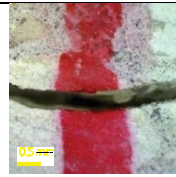
Additionally, the precipitates that formed on the surface were scratched, and they were collected for X-ray diffraction (XRD) analysis.

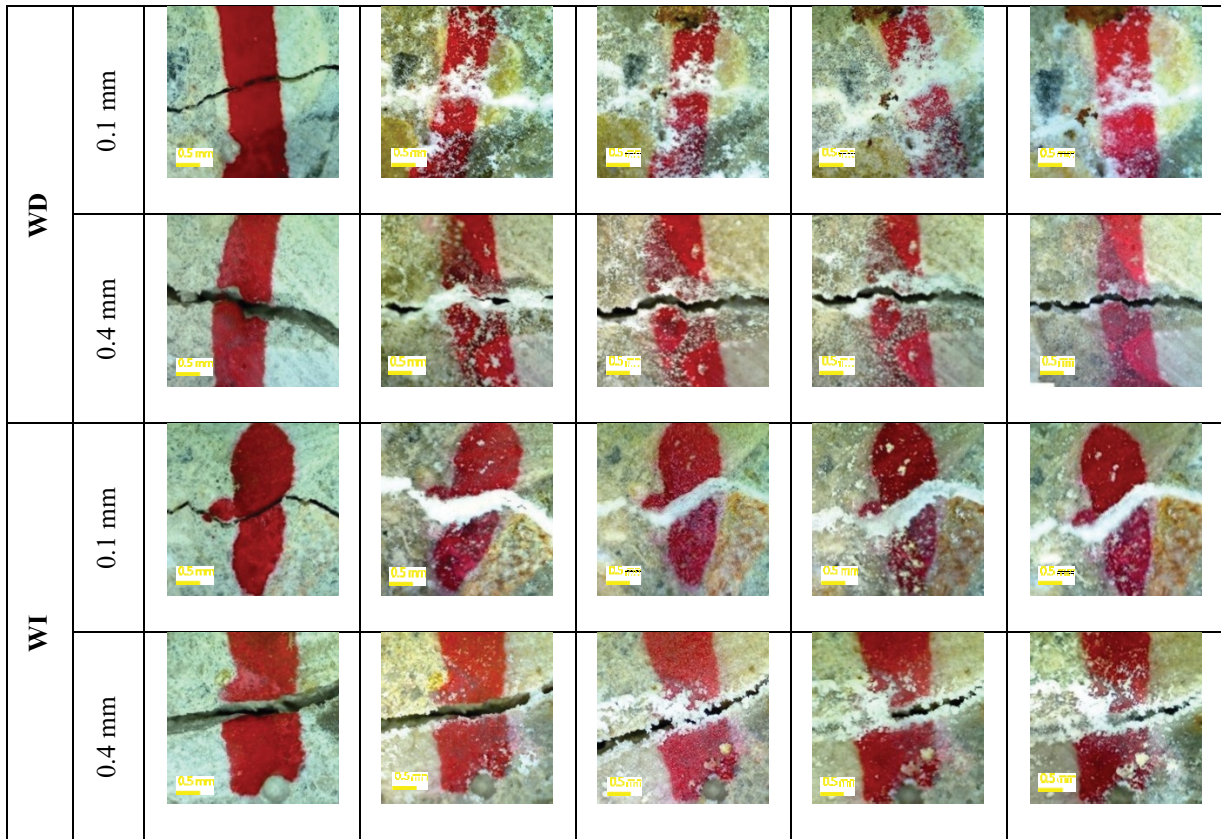
3.0 Result and Discussion

3.1. Formation of precipitates

Figure 3 shows how cracks with widths of 0.1 and 0.4 mm changed visually as they healed under the various settings examined.

Figure 3: Examples of Crack Closing Evolution for Each Case Studied. HC: Humidity Chamber; WD: Wet/Dry Cycle; WI: Water Immersion

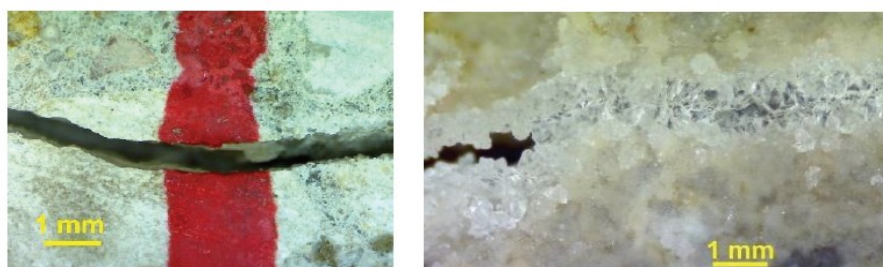
		Healing time				
		0 days	7 days	14 days	28 days	42 days
HC	0.1 mm					
	0.4 mm					



The results demonstrate that specimens housed in a humidity room did not mend, whereas specimens exposed to wet/dry cycles and water immersion completely healed microscopic fissures (0.1 mm). High crack closing rates were seen for cracks that were 0.4 mm wide, with specimens that were treated in water immersion producing the highest results.

In numerous major cracks from specimens that healed under water immersion, teeth-like precipitates were visible with a different visual appearance than surface precipitates. Two 0.4 mm cracks are shown in Figure 4 along with details about them. The specimen on the left shot was removed from it and maintained in a humidity chamber; it showed no evidence of precipitate formation. The right image, which was taken from a specimen that had been healed under water immersion, showed precipitates in the specimen's surface and interior (close to the surface).

Figure 4: Zoom of a Specimen with a 0.4 mm Crack Stored in a Humidity Chamber for 42 Days (Left) and Detail of Crystals Formed in a Specimen Healed in Water Immersion During 42 Days (Right)



According to XRD analyses, the surface-scratching precipitates were predominantly composed of calcite and brucite, the two principal compounds that were also noted in the literature. It was not surprising that brucite was found because prior investigations have found brucite in specimens exposed to cyclic exposures and magnesium may be found in trace levels in cement and limestone powder [14]. These results suggest that the self-healing of the two-day fissures under investigation can be predominantly attributed to carbonation.

3.2 Crack closing

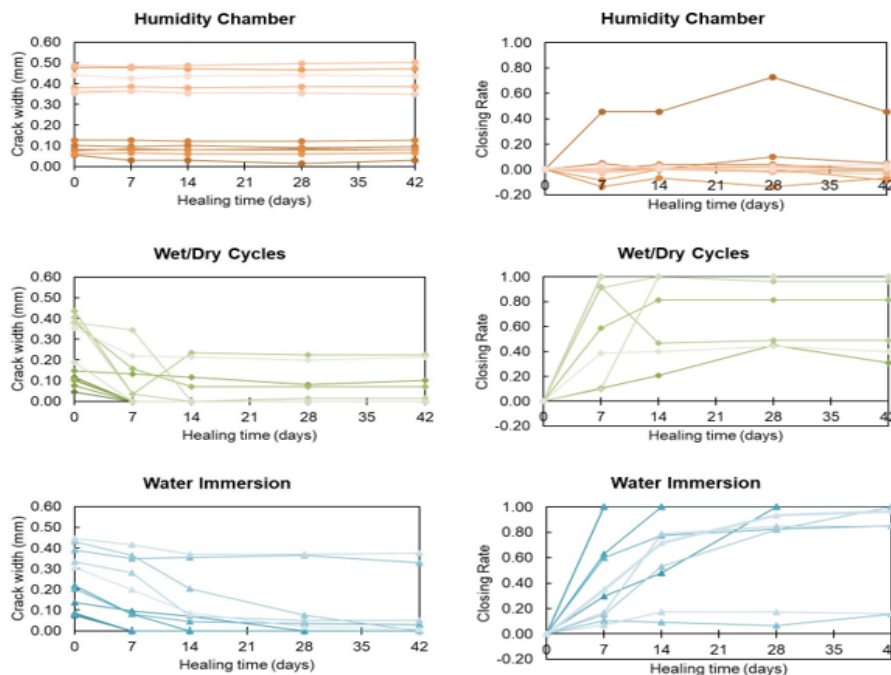
The techniques mentioned in Section 2.3 were used to measure and assess the crack width of each of these specimens.

The 12 cracks that were examined are depicted in Figure 5's (left column) evolution of crack closing for each of the three exposures: top row for the humidity chamber, middle row for wet/dry cycles, and bottom row for immersion in water.

The findings demonstrate that fractures kept in the humidity chamber exhibited stable behaviour, demonstrating that this condition did not cause precipitates to form in the cracks, and demonstrating that fluctuations in crack width were caused by measurement error. Specimens that had undergone wet/dry cycles healing had precipitates form quickly in the crack for up to 14 days before stabilising. On the other hand, even after that, the precipitates' development reduced the fracture width in specimens that had healed under water immersion. Even when submerged in water, cracks wider than 0.42-0.45 mm were too wide to begin precipitate production and the crack-closing process.

Between the measurements collected at the seventh and fourteenth days of healing, one of the fissures exposed to wet/dry cycles underwent a certain amount of reopening. The crack was sealed as a result of part of the precipitates being separated, which could have happened due to handling during the introduction and removal from water operations. This feature raises the possibility that the precipitates created during the initial stages of healing may not be firmly bonded to the matrix.

Figure 5: Evolution of Crack Width (Left Column) and Crack Closing Rate (Right) for the Three Exposures

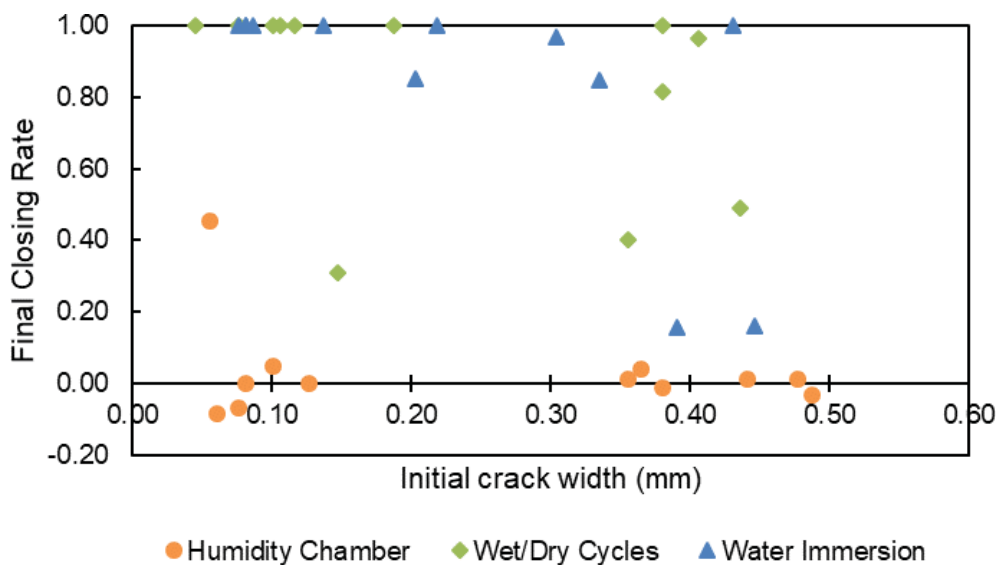


In the right column of Figure 5, the results calculated using the crack closing rate mentioned in Equation are shown. (1). The specimen that had been cured in a humidity chamber showed some dispersion in this case, while the remaining values ranged by roughly zero. This dispersion was produced in the crack with the lowest size due to the expression's division of two small values and the method's lack of precision. For specimens healing during wet/dry cycles and submersion in water, the results from this parameter gave the same information as the crack closing evolution.

By analysing the end values of the crack closing rates based on the original crack width of the specimens in the humidity chamber, it is feasible to confirm that they may be used as the control group and that the specimens did not heal, regardless of their original crack width (Figure 6). Wet/dry cycles and water immersion were used to accomplish complete crack closing for specimens with cracks less than 0.15 mm and usually good crack closing for specimens with cracks between 0.15 and 0.35 mm. However, the rate of crack closing considerably decreased for larger cracks. Smaller cracks self-close more quickly than larger cracks, as has already been mentioned.

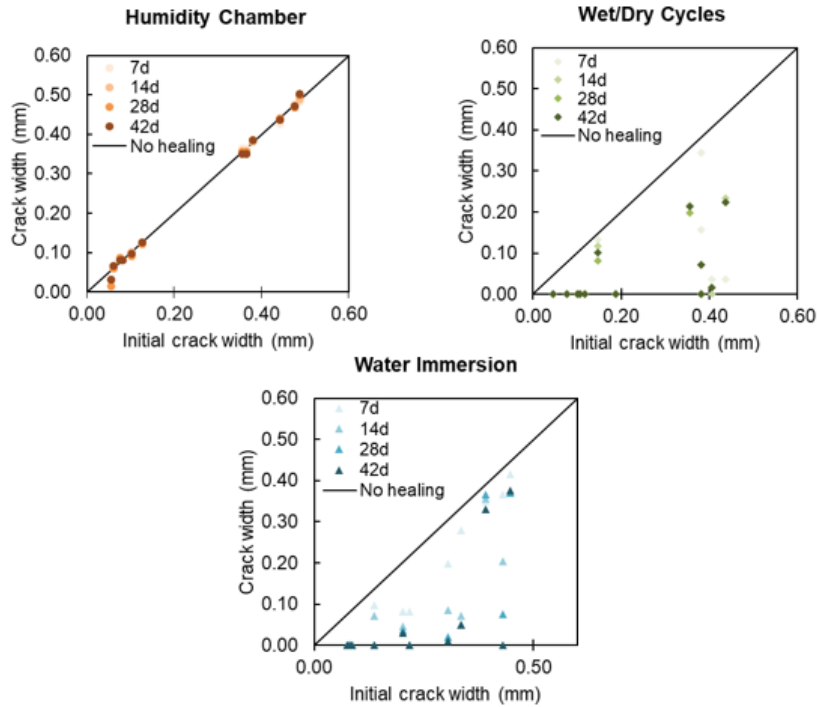
written works [4,11,14]. The data do not demonstrate a minimal threshold fracture width that must be obtained in order for the water necessary for the reactions to enter more easily, as reported by other studies [19,25]. The authors of [15] theorised that the method's precision constraints are what are to blame for this outcome. Cracks longer than 300 mm did not exhibit significant crack closing, and they are unlikely to do so even after being submerged in water for a year [8], which is consistent with the findings in [8,9], [8,9], and [8].

Figure 6: Final crack Closing Rate after 42 Days of Healing Depending on the Initial Crack Width



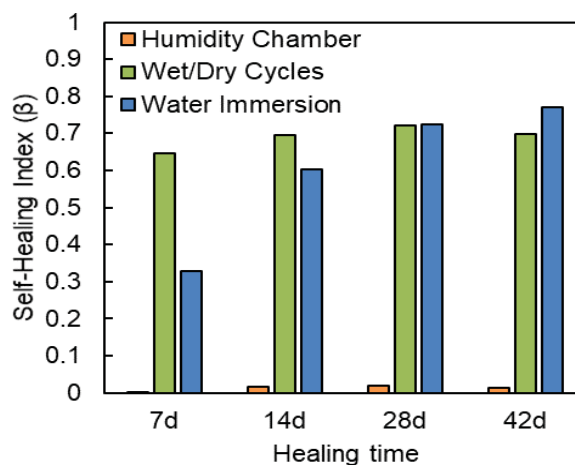
Similar conclusions can be drawn when crack width is displayed in the vertical axis in relation to the original crack width in the horizontal axis (Figure 7). These figures show that the whole distribution of specimen healing points in the humidity chamber is centred around the "no healing" bisecting line. The wet/dry cycle and water immersion scenarios both include points that are close to the horizontal axis, indicating that the crack is closing.

Figure 7: Representation of Crack Width at Each Healing Time Considered (Vertical Axis) Compared with the Initial Crack Width (Horizontal Axis)



Equation is used to compute the self-healing index of fracture closure using the graphs in Figure 7. (2). The results of this self-healing index of fracture closure are shown in Figure 8. This graph demonstrates that specimens that underwent wet/dry cycles healed far more quickly than ones that underwent water immersion. This speed of healing remained at an efficiency of about 65 to 72 percent, whereas specimens healing under water immersion demonstrated enhanced fracture sealing even after 28 to 42 days of healing. After 42 days of mending in the water, this concrete with early-age cracks had only achieved its maximum efficiency at 77 percent.

Figure 8: Self-Healing Index of Crack Closing for Concrete Healing Under the Three Selected Conditions



Edvardsen [4] has already proposed that an efficiency limit should exist for autogenous healing brought on by carbonation because of the two-phase process discussed in Section 1. The apparent inconsistencies in the literature about the best healing condition are clarified by this finding. Wet/dry cycles, as opposed to continuous immersion in water, have been demonstrated to generate better outcomes in certain studies [17,26], which appeared to be at variance with the results of other investigations, which found that specimens behaved better when immersed in water [14,15]. This apparent disagreement could be caused by the diverse evaluation methods and criteria. For example, [15] used early-age precracking and 42-day healing durations, but it just looked at the ultimate self-healing and neglected the evolution over time, whereas [14] published the results one year after healing. In these two cases, it was claimed that immersion in water was superior to wet/dry cycles. Contrarily, the authors of [17] proposed that after four to five cycles of water exposure, the pace of autogenous healing would begin to slow until plateauing after ten cycles (which lasted around 10 days). Their conclusions for cracks in young people are in line with those of our investigation. Older cracks might have different outcomes; in [14], for instance, the authors didn't see self-healing until the crack was submerged in water.

The points in Figure 7 show a quadratic-like trend that is more obvious for specimens healing while submerged in water but relatively diffuse for wet/dry cycles. This type of trend highlights two crucial points: At the point where the trend intersects the bisecting line that denotes "no healing," a crack width value for which autogenous healing is not possible would be obtained, and B that the maximum completely healable crack width (with 100% of the crack closing) can be obtained at the point where the trend intersects with the horizontal axis.

This work provides a basic model to quantify the self-healing generated in concrete in terms of fracture closing. This model should be able to forecast the eventual crack width for a crack of size x after a healing period t . Equation (3) is suggested to accomplish this, with y being a quadratic equation of x and possibly being affected by t through the parameters a and c , stated in Equations (4) and (3). (5). This equation guarantees that the bisecting line for $t = 0$ is the final equation. (i.e., no healing)

$$Y = \min \{ y(t - 1); \max \{ 0; a * x^2 + b * x - c \} \} \quad \dots(3)$$

Where

$$a = \beta * mt \quad \dots (4)$$

$$c = \lambda * tn \quad \dots (5)$$

These values were determined for the WD and WI circumstances, respectively, by lowering the equations' least squares errors (LSE) in relation to the research's experimental results. Three of these five criteria were fixed as local mix-setup parameters using the average of the values obtained for WD and WI because the values were very comparable across the two groups.

Table 2: Model Parameters Obtained for Wet/Dry Cycles and Water Immersion

	WD	WI
λ	0.02176	
β	1.03393	
ρ	0.80543	
n	0.74699	1.06304
m	0.57343	1.66690

To maximise the fitting correction, the model was then run a second time. As a result, we were able to develop an ideal model that depends only on two factors on the conditions of healing. Once this local optimization was completed, the three fixed parameters remained unaltered, and the conditions were lifted to allow the optimising tool to run again. Table 2 displays the values obtained for the five model parameters, with the fixed values highlighted in grey. LSE values for the WD group were 4.503 and for the WI group were 1.300, demonstrating that the specimens submerged in water fit the model more closely.

Figure 9 displays the curves that these models for specimens healing underwater and during wet/dry cycles produced. The maximum crack width for which no autogenous healing occurs to close the crack in either scenario is considered to be 0.45 mm. Furthermore, it is clear that a fracture's size increases with time and that this size increases as specimens heal underwater. A fracture is considered totally "healable" when 100% of the crack closes. For example, in specimens healing under wet/dry cycle conditions, only cracks of 0.10 mm can heal completely after 7 days, whereas this value increases to 0.16 mm under water immersion settings. Similar to this, it can be expected that only cracks 0.25 mm and smaller will completely close in the WD conditions after 42 days of healing, but cracks up to 0.32 mm may do so in the case of WI. Furthermore, the model makes no distinction between healing for 28 and 42 days, and its points for specimens that heal for 1000 days also do not significantly differ from one another. These results also show that self-healing rates in WD situations are higher over the first 28 days but that they decrease over time. Conditions where water is immersed in the cracks between 0.25 and 0.32 mm are more advantageous than wet/dry cycle settings.

The achieved standard error of regression (S) for these models is summarised in Table 3. Since the group that underwent wet/dry cycles had data that were substantially more irregular, the model's accuracy is poor. In the case of specimens healing during water immersion, lower S values were recorded, indicating improved accuracy. The obtained dispersion is roughly 0.10 mm, which is comparable to the dispersion of the experimental data.

Figure 9: Self-Healing Models for Crack Closing by Autogenous Healing in Wet/Dry (Left) and Water Immersion Conditions (Right)

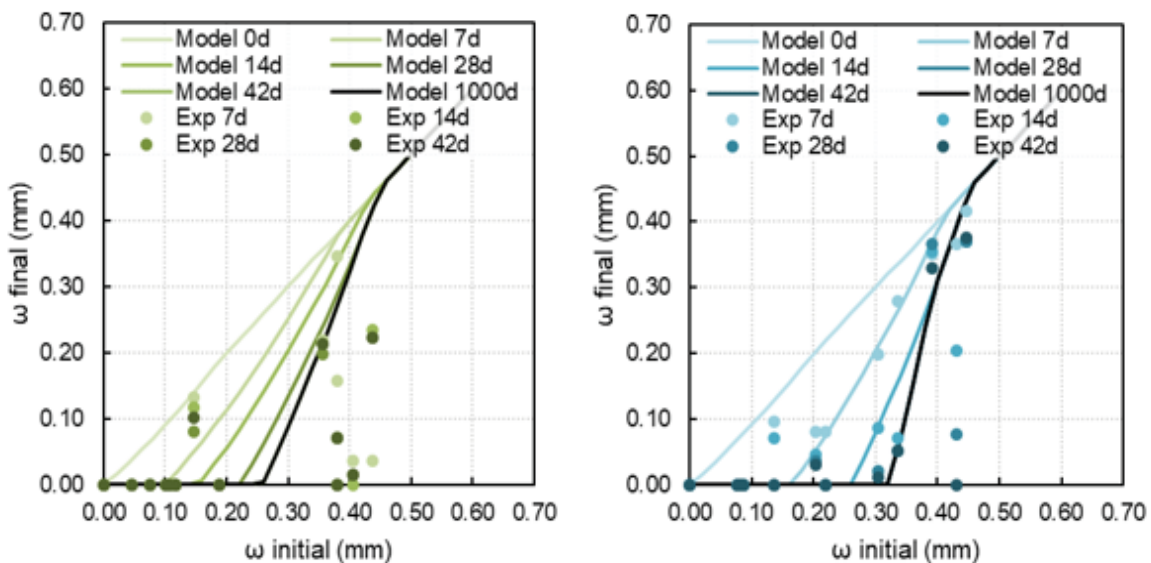


Figure 9. Self-healing models for crack closing by autogenous healing in wet/dry (left) and water immersion conditions (right).

Table 3: Standard Error of Regression (S) for All Model Curves Obtained

	S (mm)			
	7 Days	14 Days	28 Days	42 Days
WD	0.186	0.191	0.162	0.157
WI	0.038	0.073	0.101	0.121

3.3 Internal crack and carbonation

To ascertain if crack closing occurred inside the specimens, cuts transverse to the crack plane were made into the tested cylindrical specimens as explained in Section 2.4. Figure 10 shows samples with large cracks that partially healed both before and after the cut while being subjected to wet/dry cycles.

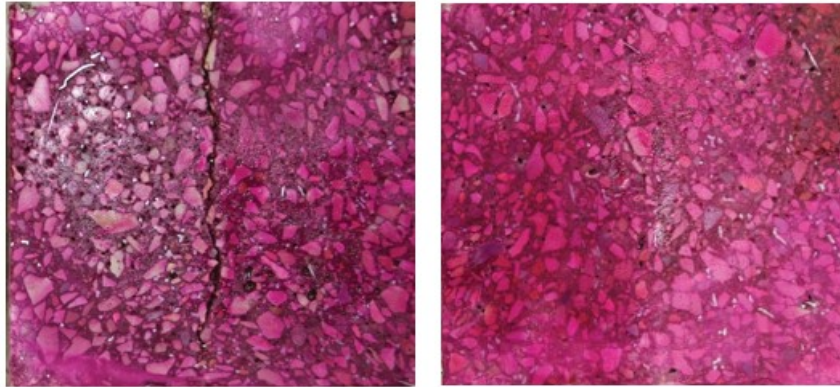
Figure 10: Surface Cracks Healed in Specimens with Large Cracks Healing under WD Cycles, and Internal Crack after Cutting the Cylinder Transversally to the Crack



Figure 10 Right illustrates the surfaces where the cut has left empty fractures, while Figure 10 Left depicts the surfaces where the fissures have totally or partially healed up (white precipitates). Small fissures, if they even existed, were difficult to see following the cut. However, due to the partial modification of the crack formed during the cut, which shows that particles were released, the internal crack width could not be measured exactly for comparison with the surface crack width. This study raises questions regarding how interior and surface crack widths impact self-healing as a whole and about the best evaluation methods for precisely quantifying self-healing.

All specimens were coloured with phenolphthalein after the cylinders were cut transversely, and the resulting sections were photographed. For fractures of a size around 0.10 mm compared to cracks of a size around 0.40 mm, the acquired sections showed no colouring changes regardless of the healing condition (under water immersion, wet/dry cycles, or being stored in humidity chamber). Figure 11 shows the cross section of two specimens, each of which has a significant crack that is around 0.4 mm in width. The specimen is seen being maintained in a humidity chamber on the left, and has been mended utilising wet/dry cycles on the right. Both regions' magenta hue indicated the absence of surfaces with carbonation. However, some parts appear to have carbonation beginning (top of the crack in Figure 11 Left), while other sections show no symptoms of carbonation (bottom part of the crack in Figure 11 Left). It should be noted that the sawing procedure might have altered the section or the appearance of the precipitates.

Figure 11: Two Examples of Tested Specimens with the Whole Section without Carbonation. The Left Picture Shows a Section of a Small Crack Specimen Stored in Humidity Chamber, the Right Picture Shows a Section of a Large Crack Specimen Healed in Wet/Dry Cycles.



In fact, additional testing on extra samples from other experimental campaigns [24], which were older and exposed to water immersion conditions for a longer period of time (a total of 6 months), revealed carbonation in the region closest to the surface (uncolored area in Figure 12), with a depth between 5 and 10 mm for all the discs tested. These results confirm the pattern found in [8], which found that the highest crack depth was 0.34 mm below the surface.

For comparison, in earlier investigations, carbonation depths of 3 mm were found after 120 days in mortars with an uncracked compressive strength of 45–50 MPa [27]. Concrete specimens examined in a different investigation employing CEM I and concrete with a comparable compressive strength (33 MPa) to this one found that it took two years of outdoor exposure before carbonation depth developed to more than 3 mm; after six years, carbonation depth was kept below 8 mm [28]. These data suggest that carbonation cannot effectively aid the internal autogenous healing of the fissures and that the process discovered mostly resulted in surface depositions that seal the crevices.

Figure 12: Sealed Disks (Left) and Broken Half of a Disk After the Phenolphthalein Test (Right)



4.0 Conclusion

This study's goal was to examine the fracture closing brought on by autogenous repair. A humid chamber, wet/dry cycles, and immersion in water as healing conditions were taken into

account, along with crack diameters of 0.1 mm and 0.4 mm. The following are the inferences that can be made:

- High humidity environments were unable to make fissures seem to seal. Wet/dry cycles and water immersion were used to completely close cracks in specimens with cracks smaller than 0.15 mm, and generally good closing was accomplished for cracks bigger than 0.15 mm. For larger cracks, the rate of crack closing was noticeably slower.
- Compared to specimens submerged in water, specimens exposed to wet/dry cycles recovered more quickly during the first seven days of healing. With a 65–72 percent overall efficiency, the healing process slowed after 7 days of wet/dry cycles. The crack closing under water immersion, on the other hand, continued after the first seven days and, after 42 days of healing, reached a global efficiency of 77 percent.
- A fundamental model was proposed to predict crack closing in concrete in order to quantify the residual crack width for a certain initial crack. The curves the model generated show an increase in "healable" crack width with healing time (with 100% of the fracture closed). Fractures measuring 0.10 mm could be healed after seven days of healing in wet/dry cycles, but cracks measuring 0.16 mm could be sealed after the same length of time in water immersion. Similar to this, after 42 days of healing, their values climbed to 0.25 mm (wet/dry) and 0.32 mm (water immersion). In this experiment's conditions, autogenous healing did not take place in cracks greater than 0.45 mm.
- Surface fissures were repaired by autogenous healing; however, the inside of the crevices was mainly empty. The precipitates that formed were calcite and brucite, by-products of carbonation, but phenolphthalein and visual examination of the specimens showed that there was no evidence of internal carbonation.

References

1. Rooij, M.; van Tittelboom, K.; Belie, N.; Schlangen, E. *Self-Healing Phenomena in Cement-Based Materials: State-of-the-Art Report of RILEM Technical Committee*; Springer: Dordrecht, The Netherlands, 2013; ISBN 9400766246.
2. De Belie, N.; Gruyaert, E.; Al-Tabbaa, A.; Antonaci, P.; Baera, C.; Bajare, D.; Darquennes, A.; Davies, R.; Ferrara, L.; Jefferson, T.; et al. A Review of Self-Healing Concrete for Damage Management of Structures. *Adv. Mater. Interfaces* 2018, 5, 1800074.
3. Van Tittelboom, K.; De Belie, N. Self-healing in cementitious materials-a review. *Materials (Basel)* 2013, 6, 2182–2217.
4. Edvardsen, C. Water permeability and autogenous healing of cracks in concrete. *ACI Mater. J.* 1999, 96, 448–454.
5. Yuan, L.; Chen, S.; Wang, S.; Huang, Y.; Yang, Q.; Liu, S.; Wang, J.; Du, P.; Cheng, X.; Zhou, Z. Research on the improvement of concrete autogenous self-healing based on the regulation of cement particle size distribution (PSD). *Materials (Basel)*. 2019, 12, 2818.
6. Gagné, R.; Argouges, M. A study of the natural self-healing of mortars using air-flow measurements. *Mater. Struct. Constr.* 2012, 45, 1625–1638.

7. Kumar, K. Sharma, and A. R. Dixit, "Role of graphene in biosensor and protective textile against viruses," *Medical Hypotheses*, vol. 144, p. 110253, Nov. 2020, doi: 10.1016/J.MEHY.2020.110253.
8. Suleiman, A.R.; Nehdi, M.L. Effect of environmental exposure on autogenous self-healing of cracked cement-based materials. *Cem. Concr. Res.* 2018, *111*, 197–208.
9. Jaroenratanapirom, D.; Sahamitmongkol, R. Self-crack closing ability of mortar with different additives. *J. Met. Mater. Miner.* 2011, *21*, 9–17.
10. Schlangen, E.; Ter Heide, N.; van Breugel, K. Crack healing of early age cracks in concrete. In *Measuring, Monitoring and Modeling Concrete Properties*; Springer: Dordrecht, The Netherlands, 2007.
11. Qian, S.; Zhou, J.; de Rooij, M.R.; Schlangen, E.; Ye, G.; van Breugel, K. Self-healing behavior of strain hardening cementitious composites incorporating local waste materials. *Cem. Concr. Compos.* 2009, *31*, 613–621.
12. Yıldırım, G.; Khiavi, A.H.; Yesilmen, S.; Sahmaran, M. Self-healing performance of aged cementitious composites. *Cem. Concr. Compos.* 2018, *87*, 172–186.
13. Rajczakowska, M.; Habermehl-Cwirzen, K.; Hedlund, H.; Cwirzen, A. The Effect of Exposure on the Autogenous Self-Healing of Ordinary Portland Cement Mortars. *Materials (Basel)* 2019, *12*, 3926.
14. Fagerlund, G.; Hassanzadeh, M. *Self-Healing of Cracks in Concrete Long-Term Exposed to Different Types of Water*; Division of Building Materials, LTH, Lund University: Lund, Sweden, 2010; ISBN 4646222442.
15. Roig-Flores, M.; Pirritano, F.; Serna, P.; Ferrara, L. Effect of crystalline admixtures on the self-healing capability of early-age concrete studied by means of permeability and crack closing tests. *Constr. Build. Mater.* 2016, *114*, 447–457.
16. Yang, Y.; Lepech, M.D.; Yang, E.H.; Li, V.C. Autogenous healing of engineered cementitious composites under wet-dry cycles. *Cem. Concr. Res.* 2009, *39*, 382–390.
17. Yang, Y.; Yang, E.H.; Li, V.C. Autogenous healing of engineered cementitious composites at early age. *Cem. Concr. Res.* 2011, *41*, 176–183.
18. Liu, H.; Huang, H.; Wu, X.; Peng, H.; Li, Z.; Hu, J.; Yu, Q. Effects of external multi-ions and wet-dry cycles in a marine environment on autogenous self-healing of cracks in cement paste. *Cem. Concr. Res.* 2019, *120*, 198–206.
19. Van Tittelboom, K.; Gruyaert, E.; Rahier, H.; De Belie, N. Influence of mix composition on the extent of autogenous crack healing by continued hydration or calcium carbonate formation. *Constr. Build. Mater.* 2012, *37*, 349–359.

20. Huang, H.; Ye, G.; Damidot, D. Effect of blast furnace slag on self-healing of microcracks in cementitious materials. *Cem. Concr. Res.* 2014, *60*, 68–82.
21. Wiktor, V.; Jonkers, H.M. Quantification of crack-healing in novel bacteria-based self-healing concrete. *Cem. Concr. Compos.* 2011, *33*, 763–770.
22. Snoeck, D.; De Belie, N. Mechanical and self-healing properties of cementitious composites reinforced with flax and cottonised flax, and compared with polyvinyl alcohol fibres. *Biosyst. Eng.* 2012, *111*, 325–335.
23. Ferrara, L.; Van Mullem, T.; Alonso, M.C.; Antonaci, P.; Borg, R.P.; Cuenca, E.; Jefferson, A.; Ng, P.-L.; Peled, A.; Roig-Flores, M.; et al. Experimental characterization of the self-healing capacity of cement based materials and its effects on the material performance: A state of the art report by COST Action SARCOS WG2. *Constr. Build. Mater.* 2018, *167*, 115–142.
24. Hemant singh Parihar, Prakash Singh, Prashant Sharma, Neha Sharma, Yogendra Kumar, “Exploring the Effects of Stearic Acid in Terms of Setting Time and Compressive Strength as an Admixture in Cement Mortar,” *Test Engineering and Management*, vol. May-June, pp. 23116–23120, 2020.
25. Zhong, W.; Yao, W. Influence of damage degree on self-healing of concrete. *Constr. Build. Mater.* 2008, *22*, 1137–1142.
26. Sisomphon, K.; Copuroglu, O.; Koenders, E.A.B. Effect of exposure conditions on self healing behavior of strain hardening cementitious composites incorporating various cementitious materials. *Constr. Build. Mater.* 2013, *42*, 217–224.
27. Argiz, C.; Menéndez, E.; Moragues, A.; SanjuAn, M.A. Recent advances in coal bottom ash use as a new common Portland cement constituent. *Struct. Eng. Int. J. Int. Assoc. Bridg. Struct. Eng.* 2014, *24*, 503–508.
28. Czarnecki, L.; Woyciechowski, P. Concrete carbonation as a limited process and its relevance to concrete cover thickness. *ACI Mater. J.* 2012, *109*, 275–282.
29. M. Verma, N. Sharma, P. Sharma, and P. Singh, “Evaluate the Effect in Terms of Setting Time and Compressive Strength of Oleic Acid as an Admixture in Cement,” *Test Engineering and Management*, vol. May-June, no. 23116, pp. 12422–12427, 2020.
30. Mausam, K., Kumar Singh, P., Sharma, K., & Gupta, R. C. (2016). Investigation of Process Parameter of EDM using Genetic Algorithm (GA) Approach for Carbon Fiber based Two Phase Epoxy composites. *Materials Today: Proceedings*, *3*(10), 4102–4108. <https://doi.org/10.1016/J.MATPR.2016.11.081>